Theoretical analysis of the operating regime of a passively-mode-locked fiber laser through nonlinear polarization rotation

Andrey Komarov,* Hervé Leblond, and François Sanchez
Laboratoire POMA, UMR 6136, Université d'Angers, 2 Bd Lavoisier, 49000 Angers, France
(Received 1 September 2005; published 22 December 2005)

The dynamics of a fiber laser passively mode-locked through nonlinear polarization rotation is theoretically investigated. The model is based on an iterative equation for the nonlinear polarization rotation and the phase plates and on a scalar differential equation for the gain, the Kerr nonlinearity, and the dispersion. It is demonstrated that depending on the orientation of the phase plates, the laser can be continuous, mode-locked, or *Q*-switched. In the latter case, an additional equation for the gain dynamics must be taken into account. Hysteresis dependence of the operating regime versus the orientation angles of the phase plates is shown. A large bistability domain between the *Q*-switch and the continuous regimes is demonstrated. This model allows us to obtain the main features observed in passively-mode-locked fiber lasers.

DOI: 10.1103/PhysRevA.72.063811 PACS number(s): 42.60.Fc, 42.65.Sf

I. INTRODUCTION

Self-started, passively-mode-locked fiber lasers are very attractive from the dynamical point of view because they exhibit a large variety of behaviors. Indeed, in addition to the regular mode-locking regime which has been reported in different optical configurations, many regimes involving several pulses by cavity round trips have been experimentally observed or theoretically predicted [1–6]. Other features such as the *Q*-switch operation and bistability between the continuous (cw) and mode-locked or *Q*-switch regimes were also reported [3,5]. Many of the experimental configurations involve some phase plates. Hysteresis phenomena as a function of the orientation of the phase plates have been also reported [7]. In this paper we are interested in fiber lasers passively mode-locked through nonlinear polarization rotation. The principle is based on the rotation of the polarization ellipse resulting from the optical Kerr nonlinearity [8]. A unidirectional ring cavity is considered together with a polarizer placed between two polarization controllers. If, at the output of the fiber, the polarization controller is suitably adjusted, the polarizer lets the center of the pulse pass while it blocks the low-intensity wings [4,9,10]. Although there are many theoretical papers devoted to the mode-locking through nonlinear polarization rotation, most of them are focused on a particular behavior. In addition, the phase plates are not directly taken into account and therefore their effects on the operating regime of the fiber laser cannot be described. However, Haus *et al.* [11] had considered analytically the nonlinear losses resulting from nonlinear polarization rotation combined with a polarization controller and a polarizer. The calculated approximate nonlinear loss parameter explicitly takes into account the coefficient of the matrix associated with the polarization controller. An attempt to explicitly include the orientation angles of the phase plates has been recently reported in [12]. The model reduces to a scalar cubic complex Ginzburg-Landau equation. The coefficients explicitly depend on the orientation of the phase plates. The great advantage of this model is that it allows us to investigate analytically the stability of the mode-lock and the continuous solutions as a function of the orientation angles of the phase plates [12–14]. Its major drawback is that it does not take into account gain saturation. As a consequence, hysteresis phenomena cannot be obtained with such an approach. In a recent paper, we have proposed a model including saturation effects together with the orientation angles of the phase plates [15]. This allowed us to successfully account for multiple pulsing behavior as well as hysteresis phenomena versus the pumping power.

The aim of this paper is to show that our recent model is able to reproduce the key features exhibited by a passively-mode-locked fiber laser: bistability between the cw and the mode-lock or *Q*-switch regimes, hysteresis as a function of the angles, and *Q*-switching. In Sec. II we briefly present the model and the numerical procedure. Section III is devoted to numerical results. Bistability between the mode-locked and the cw regime is first shown and also multiple pulsing behavior. Large hysteresis phenomenon versus the phase plate orientation is pointed out. In Sec. IV, the model is modified to take into account the finiteness of the relaxation time of the gain, which is needed to describe the *Q*-switching operation. The resulting three-equation model is able to reproduce cw, *Q*-switch, and mode-lock regimes as well as bistability between the different regimes. Different unstable behaviors are also demonstrated.

II. THE MODEL

We consider a ytterbium-doped fiber ring laser operating in the normal dispersion regime and passively mode-locked through nonlinear polarization rotation. The setup is schematically shown in Fig. 1. For isotropic fibers this scheme involves all necessary elements for the control of nonlinear losses. After the polarizing isolator the electric field has a linear polarization. Such states of polarization do not expe-

*Permanent address: Institute of Automation and Electrometry, Russian Academy of Sciences, Acad. Koptyug Pr., 1, 630090 Novosibirsk, Russia.

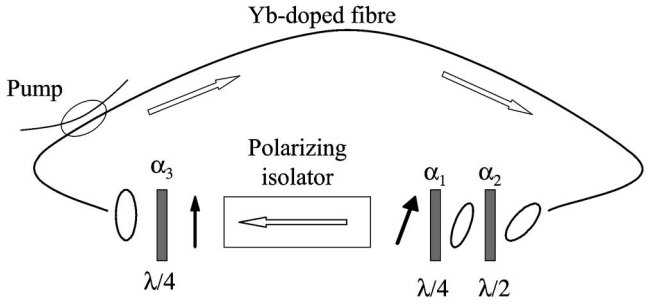

FIG. 1. Schematic representation of a fiber laser passively mode-locked through nonlinear polarization rotation.

rience polarization rotation in the fiber because the rotation angle is proportional to the area of the polarization ellipse. Consequently, it is necessary to place a quarter-wave plate 3 (α_3 represents the orientation angle of one eigenaxis of the plate with respect to the laboratory frame). At the output of the fiber, the direction of the elliptical polarization of the central part of the pulse can be rotated towards the passing axis of the polarizer by the half-wave plate 2 (the orientation angle is α_2). Then this elliptical polarization can be transformed into a linear one by the quarter-wave plate 1 (the orientation angle is α_1). In this situation the losses for the central part of the pulse are minimum while the wings undergo strong losses. The setup of Fig. 1 has been modeled as follows [15]. The fiber has been assumed to have group velocity dispersion (GVD), optical Kerr nonlinearity, and saturable gain. Linear birefringence has not been taken into account in our model since it is not required for mode locking neither for hysteresis phenomena. The nonlinear losses are described by solving, in a first step, the equations for a field propagating in a Kerr medium when dispersion is neglected, and then taking into account the three phase plates and the polarizer (self- and cross-phase-modulation terms were considered together with four-wave mixing terms). On the other hand, a scalar equation has been written for a wave propagating in a saturable amplifying medium with GVD, to account for dispersion and gain. The resulting model assumes localized effects for the nonlinear loss due to the Kerr nonlinearity and the phase plates, while gain and GVD are distributed. In a dimensionless form, the final set of equations for the electric field amplitude is

$$\frac{\partial E}{\partial \zeta} = (D_r + iD_i)\frac{\partial^2 E}{\partial \tau^2} + (G + i|E|^2)E, \tag{1}$$

$$E_{n+1}(\tau) = -\beta[\cos(pI_n + \alpha)\cos(\alpha_1 - \alpha_3) + i\sin(pI_n + \alpha)\sin(\alpha_1 + \alpha_3)]E_n(\tau), \tag{2}$$

where $\zeta = z/L$, $\tau = t/\delta t$, $G = a/(1 + b\int I\, d\tau)$, $D_r = GD_r^0 + d_r$, $D_r^0 = 2/(|\beta_2|L\omega_g^2)$, $I_n = |E_n|^2$, $d_r = 2\rho_c/|\beta_2|$, $p = B\sin 2\alpha_3$, $a = g_0 L$, $b = I_r \delta t/(P_{sat}T_a)$, $I_r = 1/\gamma L$, $\alpha = 2\alpha_2 - \alpha_1 - \alpha_3$, and $\delta t = \sqrt{\beta_2 L/2}$.

γ ($W^{-1}\,m^{-1}$) is the nonlinear coefficient related to the nonlinear index coefficient n_2, and $B = \frac{1}{3}$ for silicate fibers [16]. β is the transmission coefficient of the polarizer (free parameter). β_2 ($ps^2\,m^{-1}$) is the second order GVD. $T_a = Ln_0/c$ (s) is the photon round trip time, n_0 the refractive index, c the velocity of light in the free space, g_0 (m^{-1}) the unsaturated gain, and P_{sat} (W) the saturating power. $P_{sat} = (h\nu\pi r^2)/(\sigma T_1)$, where $h\nu$ (J) is the photon energy, σ (m^2) the stimulated emission cross section, T_1 (s) the lifetime of the upper level of the lasing transition, and r (m) the radius of the fiber core; ν is the optical frequency and h the Planck's constant. ω_g (s^{-1}) is the spectral gain bandwidth. ρ_c describes the frequency-dependent loss due to both additional spectrally selective elements for control of a radiation spectrum or uncontrolled spectrally selective losses related with intracavity elements. D_i and L (m) are the dispersion and the length of the fiber, respectively.

The numerical procedure starts from the evaluation of the electric field after passing through the Kerr medium, the phase plates, and the polarizer, using Eq. (2). The resulting electric field is then used as the input field to solve Eq. (1) over a distance L, using a standard split-step Fourier algorithm. The computed output field is used as the new input for Eq. (2). This iterative procedure is repeated until a steady state is achieved.

III. MULTIPLE PULSING AND BISTABILITY

For the numerical simulations we consider the practical case of a ytterbium-doped fiber laser operating in the normal dispersion regime. The values of the different parameters are $\gamma = 3\times10^{-3}\ W^{-1}\,m^{-1}$ [16], $L = 9$ m, $c = 3\times10^8\ ms^{-1}$, $\beta_2 = 0.026\ ps^2\,m^{-1}$ [17], $\omega_g = 10^{13}\ s^{-1}$ [17], $r = 7\times10^{-6}$ m, $\sigma = 2.5\times10^{-24}\ m^2$, $T_1 = 8\times10^{-4}$ s, and $\beta = 0.95$.

A. Multiple pulsing and hysteresis phenomena

Before we present the results, it is of importance to discuss the effects of the different mechanisms affecting the emergence of the mode-locked regime. Equation (2) is related to the nonlinear feedback. Mode-locking requires positive feedback, i.e., the greater intensities must undergo the lower losses. In practice, the feedback is controlled by changing the orientation of the phase plates. An additional mechanism of feedback must be taken into account. Indeed, the intensity-dependent phase modulation leads to a spectral broadening and then to a lower amplification because of the finite spectral gain bandwidth. This phenomenon can be viewed as a negative feedback. The competition between these two mechanisms is responsible for bistability and hysteresis behaviors [15].

To illustrate this competition, we have numerically solved Eqs. (1) and (2) for the same values of the parameters but with different initial conditions. Results are shown in Fig. 2 which are taken from [15]. It can be seen that bistability between the cw and the mode-locked regimes is obtained. With suitable initial conditions, the positive feedback is achieved and mode-locking occurs [Fig. 2(a)]. On the other hand, when using parameters for small peak intensity, the nonlinear losses act as a negative feedback; the pulses decrease and the cw operation is reached after transient evolution. This bistability has been experimentally observed in many fiber lasers passively mode-locked through nonlinear

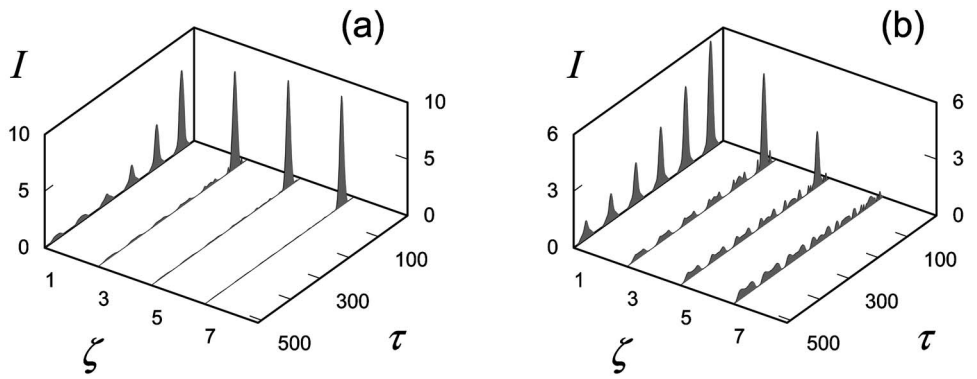

FIG. 2. (a) Mode-locking versus (b) cw operation. The parameters used are $a=2$, $\alpha=1.3$, $\alpha_1=0$, $\alpha_3=0.2$ and $D_r=0.2$.

polarization rotation [5,7]. Another feature commonly observed is the multiple pulsing regime. Indeed, under a suitable orientation of the phase plates, the laser can deliver bunches of pulses and the number of pulses increases when the pump power increases [5]. This point has been deeply investigated in our previous paper [15]. However, for completeness, we show in Fig. 3 an example of a bunch of three pulses (extracted from [15]). The analysis reported in [15] show that the number of pulses exhibits a strong pump power hysteresis and that the pulses are created and annihilated one by one.

B. Hysteresis versus the orientation of the phase plates

Let us now consider the effects of the rotation of the phase plates on the operating regime of the fiber laser. It is well established that large hysteresis occurs in passively-mode-locked fiber lasers when one phase plate is rotated. In particular, bistability between the cw and the mode-locked regime is commonly observed [5,7]. Although the analytic model developed in [12] takes into account the orientation of the phase plates, it was not possible to state about any bistable behavior. In the framework of the model based on Eqs. (1) and (2), numerical integrations allow us to point out bistability behaviors and hysteresis phenomena. Results are given in Fig. 4, which gives the evolution of the operating regime as a function of the angle α. The orientations of the phase plates numbers 1 and 3 are fixed and the half wave plate 2 is rotated in the right-hand and then in the left-hand direction. Results of Fig. 4 show that the laser is first continuous and then switches towards the mode-locked regime for $\alpha=\alpha_{ML}$ for which a positive nonlinear feedback occurs. At this stage, if the phase plate is rotated in the opposite direction, the laser becomes again a cw but for a lower value of α. A large bistability domain is then obtained versus the orientation angle of the phase plates. In addition, when the laser is in the ML regime, the number of pulses N increases when the phase plate is rotated; pulses appear one by one. Again, large hysteresis is obtained versus the orientation angle.

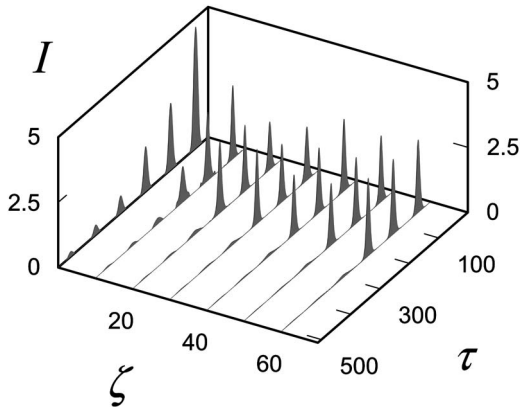

FIG. 3. Multiple pulsing operation. The parameters are the same as in Fig. 2 except for the pumping parameter $a=1.2$.

IV. SPIKE OPERATION AND PASSIVE MODE-LOCKING

A. Introduction and discussion

It is well known that solid-state lasers with saturable absorption can work in regimes of undamped spikes and of giant pulses (Q-switching operation). To model these regimes it is necessary to take into account the finiteness of the relaxation time for the gain medium.

A typical model for a solid-state laser with saturable absorption is

$$\frac{\partial I}{\partial t} = -\gamma_\ell I + \sigma N I - \sigma' N' I, \tag{3}$$

$$\frac{\partial N}{\partial t} = -\frac{N}{T_1} - \sigma N I + P, \tag{4}$$

$$\frac{\partial N'}{\partial t} = -\frac{N' - N'_0}{T_1'} - \sigma' N' I, \tag{5}$$

where γ_ℓ (s^{-1}) is the inverse of the photon lifetime, I (m^{-3}) the density of photons, N (m^{-3}) the population inversion, P (m^{-3}) the pumping, N' (m^{-3}) the population of the level responsible for the saturable absorption effect, N'_0 the value of N' at rest, T_1' (s) the lifetime of this level, and the σ's ($m^3\ s^{-1}$) are the cross sections of the corresponding transitions. Since the response time T_1' of the saturable absorber is very fast with regard to T_1 and $1/\gamma_\ell$, the so-called adiabatic approximation can be used, which leads to $N'=N'_0/(1$

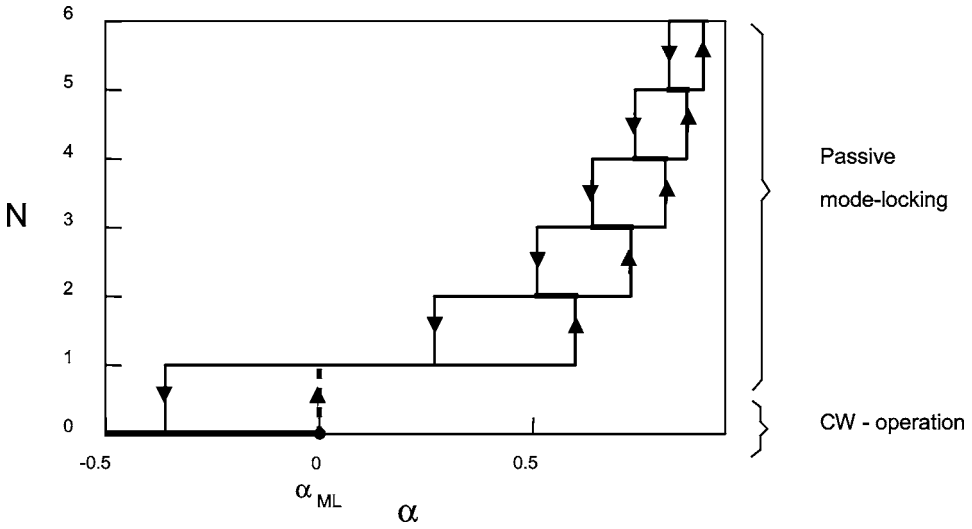

FIG. 4. Hysteresis dependence of the number of pulses in the cavity N, versus the orientation angles of the phase plates. The parameter used are $a=2$, $\alpha_1=2$, $\alpha_3=0.2$, and $D_r=0.2$. All angles are in radians.

$+\sigma'\tau' I$). In order to write down the resulting equations using the same dimensionless variables as above, we define the normalized gain as $G=\sigma T_a N/2$, a loss coefficient as $\kappa=T_a(\gamma_\ell+\sigma' N')/2$, $a=T_a\sigma\tau P/2$, and $b=\sigma\tau\delta t/T_a$. In the case of the fiber laser, it will be useful to consider the energy $J=\int I\, d\tau$. Here it is related to the intensity I assuming that the latter is constant, as $J=IT_a/\delta t$. Then Eqs. (3) and (4) reduce to

$$\dot{J}=2(G-\kappa)J, \tag{6}$$

$$\tau_g\dot{G}+(G-a)=-bGJ, \tag{7}$$

where $\tau_g=T_1/T_a$, and the dot denotes the derivative with respect to $\zeta=z/L=t/T_a$.

Let $x=\ln(J/J_{st})$ where the index "st" stands for the stationary solutions of systems (6) and (7). Combining (6) and (7) allows us to obtain an equation for x:

$$\ddot{x}+\frac{1}{\tau_g}\left(1+bJ_{st}e^x+2\frac{d\kappa}{dx}\right)\dot{x}+\frac{2}{\tau_g}[(bJ_{st}e^x+1)\kappa-a]=0. \tag{8}$$

Equation (8) is equivalent to the equation of motion of a particle in a potential well

$$U(x)=\frac{2}{\tau_g}\left[\int^x(bJ_{st}e^{x'}+1)\kappa(x')dx'-ax\right] \tag{9}$$

with the friction coefficient

$$f=\frac{1}{\tau_g}\left(1+bJ_{st}e^x+2\frac{d\kappa}{dx}\right), \tag{10}$$

which depends on x. For positive f, the particle undergoes damped oscillations in the well, which correspond to the damped spikes of the laser intensity during the transient process of the laser operation. However, due to the saturable absorber effect, N' is a decreasing function of the intensity I. Hence $d\kappa/dx$ is negative, and if it is large enough, f can be negative. Then undamped oscillations are possible, which account for Q-switching regimes.

In the case of the fiber laser, the master equations have the following form:

$$\frac{\partial E}{\partial\zeta}=(D_r+iD_i)\frac{\partial^2 E}{\partial\tau^2}+(G+i|E|^2)E, \tag{11}$$

$$E_{n+1}(\tau)=-\beta[\cos(pI_n+\alpha)\cos(\alpha_1-\alpha_3)+i\sin(pI_n+\alpha)\sin(\alpha_1+\alpha_3)]E_n(\tau), \tag{12}$$

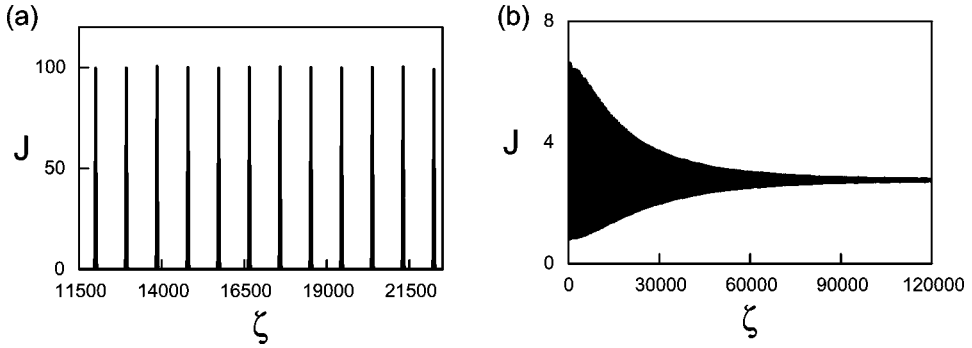

FIG. 5. Evolution of the integrated intensity J as a function of the round trip number ζ. (a) Undamped spike regime, (b) cw operation. The parameters used are $a=2.5$, $\alpha=0.1$, $\alpha_1=-1.9$, $\alpha_3=0.2$, and $D_r=0.2$. The difference exists only on initial conditions.

$$\tau_g \frac{\partial G}{\partial \zeta} + (G - a) = -Gb \int I \, d\tau. \tag{13}$$

We assume that the variations of the field in the cavity are slow enough so that the dispersion and the gain filtering can be neglected. Then it follows from Eq. (11) that the intensity evolves as $I = I(0)e^{2G\zeta}$. Equation (12), which account for the effect of the nonlinear polarization rotation and polarizer, expresses for the intensity as $I_{n+1}(0) = \eta I_n(1)$ with

$$\eta = \beta^2[\cos^2(\alpha_1 - \alpha_3) - \cos 2\alpha_1 \cos 2\alpha_3 \sin^2[pI_n(1) + \alpha]]. \tag{14}$$

$I_{n+1}(0)$, and $I_n(1)$ are the intensities at the beginning of the $(n+1)$th and at the end of the nth roundtrip, respectively. Taking into account both the gain and the nonlinear polarization rotation we get $I_{n+1}(0) = \eta I_n(0)e^{2G}$. Integrating formally Eq. (6), and comparing this expression, it is seen that J obeys an evolution equation formally identical to (6) with $\kappa = -\ln \eta/2$, η being given by (14). Since the value of the intensity involved by (14) is taken at the end of the round trip, its expression should involve the gain G. We restrict it to the case where the effect of the gain on one roundtrip is negligible, which was already assumed in the derivation of (12). Thus we take $G \approx 0$ in the expression of η, which becomes

$$\eta = \beta^2 \left[\cos^2(\alpha_1 - \alpha_3) - \cos 2\alpha_1 \cos 2\alpha_3 \sin^2\left(\frac{p\delta t}{T_a} J + \alpha \right) \right]. \tag{15}$$

Hence the laser dynamics is governed by the same systems (6) and (7) as in the case of the solid-state laser, the only difference is the expression of the losses κ as a function of the energy J.

The decrease of nonlinear losses with increasing intensity induces an additional amplification of the field in the maximum of a spike. As a result, the peak intensity becomes greater and the spikes become undamped if the nonlinear loss is large enough. The intensity of radiation in the spike regime cannot be less than the intensity of spontaneous radiation. For models, which neglect the spontaneous emission, the undamped spike operation transforms into sequences of giant pulses with a repetition rate equal to the inverse of the relaxation time of the gain. For correct description of laser operation, the spontaneous emission must be taken into account [18].

For the investigated laser, a variation of intensity $\delta I = I - I_0$ produces a variation of the transmission $\delta\eta = \eta' \delta I$ with

$$\eta' = -\tfrac{1}{2} B\beta^2 \sin 4\alpha_3 \cos 2\alpha_1 \sin 2(pI_0 + \alpha). \tag{16}$$

The nonlinear transmission η' depends on the intensity I_0. As a result, the loss nonlinearity depends also on intensity (for clarity, pI is associated to the nonlinear losses while p is the loss nonlinearity). Thus, for spike operation, the intensity is large, the loss nonlinearity is also large, and the regime of undamped spikes is realized. In the case of operation in the vicinity of the stationary regime, the peak intensity and the loss nonlinearity are small, and the regime of damped pulses is realized leading to a cw operation. This mechanism induces the dependence of the established regime on initial conditions, that is, bistability: the spike operation versus the cw regime.

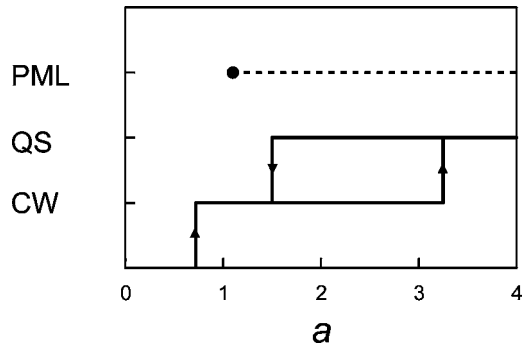

FIG. 6. Hysteresis dependence of the operating regime of the laser as a function of the pumping parameter a. The parameters used are the same as in Fig. 5. QS, Q-switch operation; PML, passive-mode-locking regime.

In the case of passive mode-locking, the peak intensity becomes very large and the negative feedback is realized: the greater intensity produces the greater losses. As a consequence, the spike becomes again damped. With a large negative feedback this damping is aperiodic. Thus, three different regimes can be realized for the same laser parameters: the cw operation, the spike operation, and passive mode-locking.

B. Results of numerical simulations

First of all we consider bistability between the cw and spike operation. This is demonstrated in Fig. 5, which represents the evolution of the integrated intensity J versus the round trip number ζ. The difference between Figs. 5(a) and 5(b) is only on the initial conditions. Hysteresis behavior on the pumping parameter is demonstrated in Fig. 6. When the laser is turned on, it is first continuous and then switches towards a Q-switch regime. The switching values of the pumping parameter are different depending on whether the pump is increased or decreased. This bistable behavior is in very good agreement with experimental results presented in Fig. 4(a) of Ref. [17] which concerns the ytterbium-doped double-clad fiber laser passively mode-locked through nonlinear polarization rotation. For the range of pumping rates investigated, the mode-locked regime is stable. However, it is not self-starting since there is no switch from the cw or spike regimes. In numerical experiments, the passive-mode-locked regime is obtained by a suitable choice of the angle α which is then adiabatically changed to its value corresponding to Fig. 6. The distribution of the field in the cavity obtained by such a procedure is shown in Fig. 7: a bunch of two pulses is shown. Although it is not possible to be exhaustive because of the great number of degrees of freedom, our results demonstrate that there is coexistence of several stable attractors and this is in very good agreement with what is observed in passively-mode-locked fiber lasers.

Other features commonly observed in passively-mode-locked fiber lasers are irregular spikes and unstable passive-

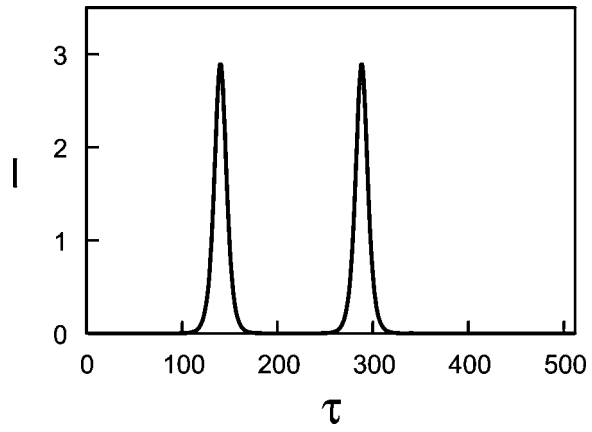

FIG. 7. Passive mode-locking obtained for $a=1.15$. The parameters used are the same as in Fig. 5.

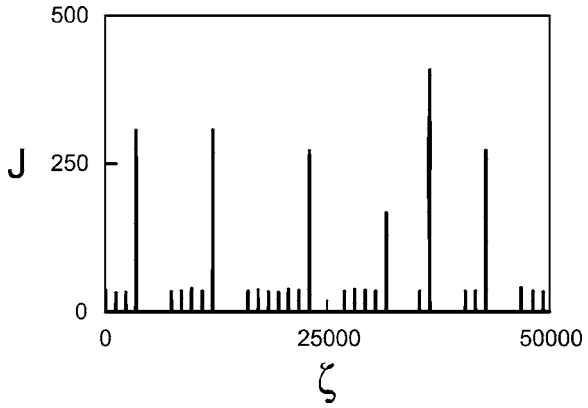

FIG. 8. Evolution of the integrated intensity as a function of the round trip number: irregular spikes. The parameters used are $a=2.1$, $\alpha=0.5$, $\alpha_1=-1.8$, $\alpha_3=0.1$, and $D_r=0.2$.

mode-locking regimes [17]. Our aim is to demonstrate that the model developed in this paper is also able to reproduce these unstable regimes. Since the stable Q-switch regime appears to be essentially incompatible with mode-locking, we have chosen parameters which are suitable for realization of passive mode-locking (when regular Q-switching is almost impossible), i.e., parameters which give the greater value for the nonlinear loss. Figure 8 demonstrates an irregular Q-switch operation. The signal consists in a train of irregular bursts containing a number of spikes varying from 1 to 12. Each burst is finished by a giant pulse in comparison with the amplitude obtained in regular spiking regime. After giant pulses we observed the extended interval during which the gain of the medium relaxes. Numerical results of Fig. 8 can be favorably compared with experimental data reported in Fig. 6 of Ref. [17]. We focus now on a distinctive feature. In the case of Fig. 8 the realization of sufficiently powerful dynamic fluctuations in spatiotemporal distribution of radiation within the cavity manifests itself as the spike with ordinary duration but with considerably greater peak intensity. In the experimental case, the peak intensity of the last spike in a sequence is standard (or slightly less) but its duration is considerably extended. This difference is explained as follows. In the experimental case, the initial power fluctuation in the spatiotemporal field distribution is a very small fraction of the total intracavity energy. As a result, the time of the increase of this fluctuation and of suppression of other field components is sufficiently large. That is, the increase of the resonator Q factor is a slow adiabatic process. Consequently, the spike is extended but its amplitude does not increase. In the case of numerical simulations we can only model a small part of the resonator (about ten ultrashort pulses). In the rest of the resonator, the field is assumed to be the same or equal to zero. As a result, the initial power fluctuation contains a considerable fraction of the total intracavity energy and hence the time of increase of this fluctuation is small, the Q factor is switched quickly, and a spike with great amplitude is realized. The nonlinear losses amplify the fluctuation in the peak intensity distribution for intracavity ultrashort pulses. In turn, these amplitude fluctuations amplify the fluctuation of the nonlinear losses. Consequently, the energy of spikes together with their amplitude are strongly affected. This process is considerably weaker in the case of laser parameters denoted in Fig. 5. For the parameters of Fig. 8, when the pumping parameter is decreased the evolution transforms into regular undamped spikes. Further decreasing a leads to cw regime after the transient behavior.

We now consider stable passive mode-locking and stationarity of average intensity. Figure 9(a) shows the transient evolution of the average intensity J as a function of the round trip number for stable passive mode-locking. Figure 9(b) shows the corresponding time distribution, which is a bunch of two pulses. Figure 10 demonstrates the evolution of the average intensity under unstable multiple pulses passive-

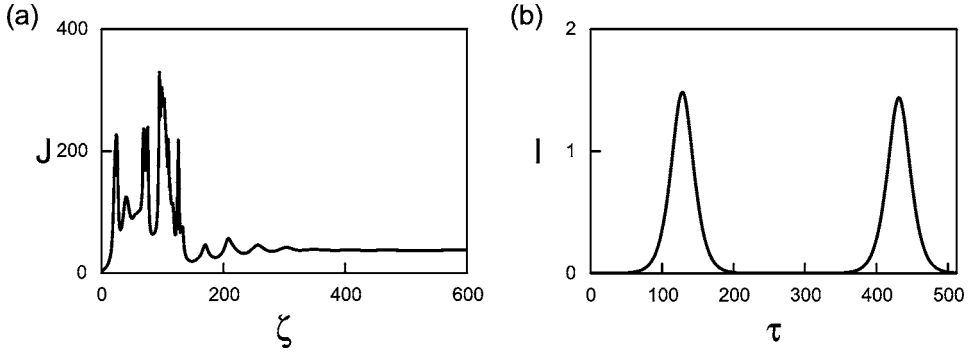

FIG. 9. (a) Evolution of the integrated intensity and (b) temporal field distribution in the passive-mode-locking regime. The parameters used are $a=2.7$, $\alpha=0.5$, $\alpha_1=-1.8$, $\alpha_3=0.1$, and $D_r=0.2$.

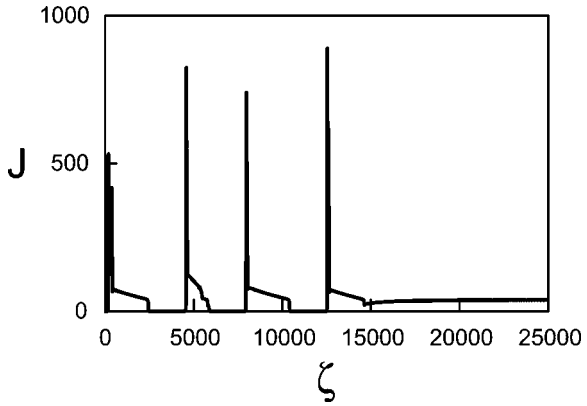

FIG. 10. Evolution of the integrated intensity J for unstable multiple pulse passive mode-locking which transforms into stable single pulse. The parameters used are $a=1$, $\alpha=0.5$, $\alpha_1=-1.8$, $\alpha_3=0.2$, and $D_r=0.2$.

mode-locking conditions. After intense spikes the multiple pulse passive mode-locking is realized. The pedestal located after the intense spike corresponds to this passive mode-locking. However, this multiple pulse passive mode-locking is unstable because the level of pumping is not high enough to support the generation of several ultrashort pulses, and hence the lasing operation is interrupted. After the relaxation of the gain this process is repeated again and again until the realization of a mode-locking with a single pulse in the cavity. After that, stable operations with single ultrashort pulse are established. For this operation, the averaged intensity J is stationary. The duration of the pedestal decreases with the increasing number of pulses in the unstable bunch state.

V. CONCLUSION

In summary, we have developed and investigated a theoretical model for a fiber laser passively mode-locked through nonlinear polarization rotation. The model takes into account the nonlinear losses resulting from the combination of the optical Kerr nonlinearity, the wave plates, and the polarizer and also, the group velocity dispersion, the saturable gain, and the finiteness of the relaxation time of the gain. The final form of the model contains three equations: one for the nonlinear losses, another one for the propagation along a dispersive and amplifying medium, and the last one, for the gain dynamics. This model allowed us to obtain the main features exhibited by passively mode-locked fiber lasers. We have demonstrated a strong hysteresis of the operating regime as a function of the orientation of the phase plates. The three different operating regimes commonly observed in such lasers have been numerically obtained: mode-locked, Q switched, and continuous. Here again, a strong multistability occurs versus the pumping parameter. Irregular spike operations and unstable passive mode-locking have been demonstrated. Our numerical results are in good agreement with typical experimental data reported in many passively-mode-locked fiber lasers.

[1] A. B. Grudinin, D. J. Richardson, and D. N. Payne, Electron. Lett. **28**, 67 (1992).
[2] M. J. Guy, D. U. Noske, and J. R. Taylor, Opt. Lett. **18**, 1447 (1993).
[3] K. Tamura, E. P. Ippen, H. A. Haus, and L. E. Nelson, Opt. Lett. **18**, 1080 (1993).
[4] V. J. Matsas, T. P. Newson, D. J. Richardson, and D. N. Payne, Electron. Lett. **28**, 1391 (1992).
[5] D. Y. Tang, W. S. Man, and H. Y. Tam, Opt. Commun. **165**, 189 (1999).
[6] N. N. Akhmediev, A. Ankiewicz, and J.-M. Soto-Crespo, Phys. Rev. Lett. **79**, 4047 (1997).
[7] B. Ortaç, A. Hideur, M. Brunel, T. Chartier, M. Salhi, H. Leblond, and F. Sanchez, Appl. Phys. B: Lasers Opt. **77**, 589 (2003).
[8] L. Dahlström, Opt. Commun. **5**, 157 (1972).
[9] D. U. Noske, N. Pandit, and J. R. Taylor, Electron. Lett. **28**, 2185 (1992).
[10] K. Tamura, H. A. Haus, and E. P. Ippen, Electron. Lett. **28**, 2226 (1992).
[11] H. A. Haus, E. P. Ippen, and K. Tamura, IEEE J. Quantum Electron. **30**, 200 (1994).
[12] H. Leblond, M. Salhi, A. Hideur, T. Chartier, M. Brunel, and F. Sanchez, Phys. Rev. A **65**, 063811 (2002).
[13] M. Salhi, H. Leblond, and F. Sanchez, Phys. Rev. A **67**, 013802 (2003).
[14] M. Salhi, H. Leblond, and F. Sanchez, Phys. Rev. A **68**, 033815 (2003).
[15] A. Komarov, H. Leblond, and F. Sanchez, Phys. Rev. A **71**, 053809 (2005).
[16] G. P. Agrawal, *Nonlinear Fiber Optics*, 2nd ed. (Academic Press, New York, 1995).
[17] A. Hideur, T. Chartier, M. Brunel, M. Salhi, C. Özkul, and F. Sanchez, Opt. Commun. **198**, 141 (2001).
[18] Y. I. Khanin, *Principles of Laser Dynamics* (Elsevier, Amsterdam, 1995).